J Comput Aided Mol Des (2010) 24:733–747
DOI 10.1007/s10822-010-9370-4

Phosphorylation and ATP-binding induced conformational changes in the PrkC, Ser/Thr kinase from *B. subtilis*

Paweł Gruszczyński · Michał Obuchowski · Rajmund Kaźmierkiewicz

Received: 25 February 2010 / Accepted: 11 June 2010 / Published online: 19 June 2010

Abstract Recent studies on the PrkC, serine-threonine kinase show that that the enzyme is located at the inner membrane of endospores and is responsible for triggering spore germination. The activity of the protein increases considerably after phosphorylation of four threonine residues placed on the activation loop and one serine placed in the C-terminal lobe of the PrkC. The molecular relationship between phosphorylation of these residues and enzyme activity is not known. In this work molecular dynamics simulation is performed on four forms of the protein kinase PrkC from *B. subtilis*—phosphorylated or unphosphorylated; with or without ATP bound—in order to gain insight into phosphorylation and ATP binding on the conformational changes and functions of the protein kinase. Our results show how phosphorylation, as well as the presence of ATP, is important for the activity of the enzyme through its molecular interaction with the catalytic core residues. Three of four threonine residues were found to be involved in the interactions with conservative motifs important for the enzyme activity. Two of the threonine residues (T167 and T165) are involved in ionic interactions with an arginine cluster from αC-helix. The third residue (T163) plays a crucial role, interacting with His-Arg-Asp triad (HRD). Last of the threonine residues (T162), as well as the serine (S214), were indicated to play a role in the substrate recognition or dimerization of the enzyme. The presence of ATP in the unphosphorylated model induced conformational instability of the activation loop and Asp-Phe-Gly motif (DFG). Based on our calculations we put forward a hypothesis suggesting that the ATP binds after phosphorylation of the activation loop to create a fully active conformation in the closed position.

Keywords Activation loop · DFG-motif · HRD-motif · Molecular dynamics · PrkC kinase · Phosphorylation

Abbreviations

ATP	Adenosine triphosphate
DFG-motif	Asp-Phe-Gly conserved kinase motif
HRD-motif	His-Arg-Asp conserved kinase motif
PASTA	Penicillin-binding protein and serine/threonine kinase associated domain
PrkCc	Catalytic domain of PrkC kinase
PrkCc-ATP	Complex of PrkCc with ATP
pPrkCc	Phosphorylated catalytic domain of PrkC kinase
pPrkCc-ATP	Complex of pPrkCc with ATP
RMSd	Root mean square deviation
RMSf	Root mean square fluctuation
SAS	Solvent-accessible surface

Introduction

The importance of protein phosphorylation in living organisms is reflected in the fact that genes encoding

P. Gruszczyński (✉)
Faculty of Chemistry, University of Gdańsk, Sobieskiego 18/19, 80-952 Gdańsk, Poland
e-mail: pawelg@chem.univ.gda.pl

P. Gruszczyński · R. Kaźmierkiewicz
Intercollegiate Faculty of Biotechnology, University of Gdańsk and Medical University of Gdańsk, Kładki 24, 80-822 Gdańsk, Poland

M. Obuchowski
Department of Medical Biotechnology, Intercollegiate Faculty of Biotechnology, Medical University of Gdańsk, Dębinki 1, 80-811 Gdańsk, Poland

protein kinase domains take 2% of eukaryotic genomes [1]. Phosphorylation on Ser/Thr/Tyr residues, restricted for a long time to eukaryotic organisms, is now well established in prokaryotes. 'Eukaryotic-like' signaling systems relying on Ser/Thr- or Tyr-protein kinases are directly involved in bacterial processes such as developmental regulation, control of cell growth, stress response, virulence, sporulation, and regulation of secondary metabolites production [2–5]. One example is a model organism, *Bacillus subtilis,* which possesses a functional eukaryotic-like Ser/Thr protein kinase, six Ser/Thr phosphatases and four Tyr phosphatases [6]. Most of these enzymes have been overproduced and purified as recombinant proteins and their biochemical parameters were established [7–11].

The first crystallographic protein kinase model (PKA [12]) revealed the active structure in a phosphorylated state. The phosphorylated residue, found in the phosphorylation segment of the PKA kinase, was stabilized by positively charged residues from the surface of the enzyme. Previously investigated structures found in the inactive state have shown that unphosphorylated activation segments can adopt a variety of conformations [13–16]. An important observation was made in 1996 implying that all kinases regulated by activation of the phosphorylation segment have a conserved arginine residue in the catalytic loop [17]. These kinases were named RD-kinases, because of the conserved RD motif (from arginine and aspartic acid residues). In eukaryotic kinases, the conserved triad of residues HRD was found [18]. The R166 (PKA numbering) supports the configuration of the activation segment linking the catalytic loop, phosphorylation site and the magnesium binding loop. The other characteristic motif is the DFG triad, placed in the N-terminus of the activation segment. It forms a polar contact with the ATP phosphates via magnesium cation or directly [19]. The DFG and two subsequent residues are called the magnesium binding loop. The structural model of the activation segment is presented in Fig. 1.

Over the past few years, substantial progress has been made in molecular dynamics and its application for studying protein kinase motions, particularly in the structural basis of protein regulation by phosphorylation. For example, computational studies applied by Groban et al. [20] demonstrated application of molecular mechanics to reproduce the known conformational change due to phosphorylation in CDK2 as well as other systems, and they explored the changes in the energy landscape due to phosphorylation. Another illustration of computational studies on structural control of kinases by phosphorylation can be found in the work of Banavali et al. [21] where targeted MD simulations were performed to analyze the transition from the inactive to active kinase conformations in Hck, showing the sequential manner by which the

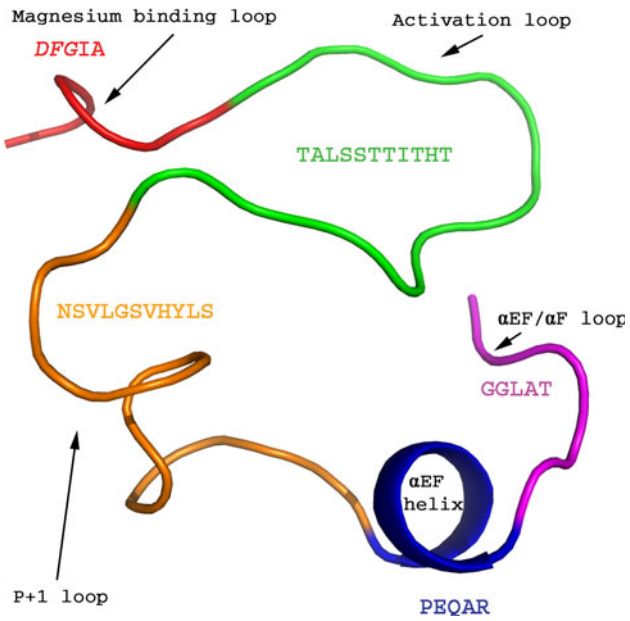

Fig. 1 An illustration of the secondary structure of PrkC activation segment presented as a cartoon model

structural effects of activation loop phosphorylation are transmitted to the catalytically crucial C-helix and to the interlobe hinge.

In this paper we investigate the structure of the catalytic domain of the PrkC, a member of the serine-threonine kinases (STPKs) from *Bacillus subtilis*. The PrkC is a membrane linked enzyme with a large extracellular domain (293 residues) containing three repeated PASTA (penicillin-binding protein and serine/threonine kinase associated domain) motifs, single membrane spanning region (27 residues) and an intracellular part built by 328 residues. The intracellular part is divided into a juxtamembrane region (59 residues) and a catalytic part consisting of 269 residues. It has been previously shown that both intracellular regions are autophosphorylated on residues three and five, respectively [4]. Recently it was shown that PrkC is located at the inner membrane of endospores and is responsible for triggering spore germination [22]. The conditions which are found inside the endospores significantly differ from those inside the vegetative cells. The water content is rather low (even 27%) in comparison to the vegetative cell (75–80%) [23]. The pH inside the dormant spores depends on the environment, however, the concentration of free hydrogen ions inside the spore can be up to three orders of magnitude higher than outside the spore [24]. In addition, ATP level is very low (less than 1% of total adenine nucleotide pool) [25].

The PrkC conformation influences the kinase activity, presumably by controlling the access of the adenosine triphosphate (ATP) and the substrate molecules to catalytic site of the enzyme. To this day, there is no crystal data

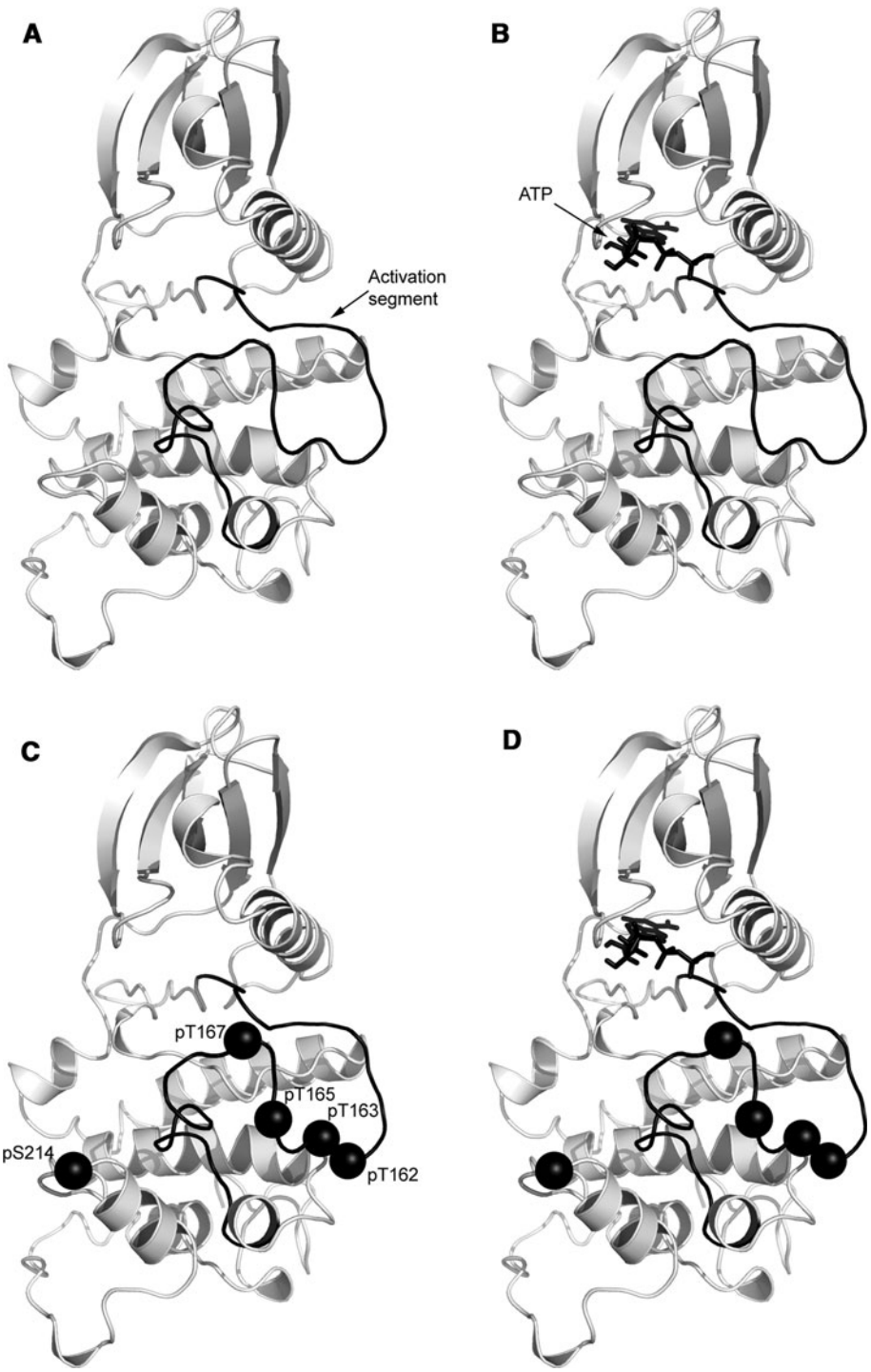

Fig. 2 Four models of PrkC catalytic domain: PrkCc (**a**), PrkCc complexed with ATP (**b**), phosphorylated PrkCc (**c**), Phosphorylated PrkCc complexed with ATP (**d**). The activation segment is presented as a *black-colored loop*. *Black spheres* represent the phosphorylated residues which are important for activity of the enzyme

concerning this kinase. Based on the primary sequence, we found characteristic residues and motifs in the PrkC kinase that are conserved in the Ser/Thr protein kinases. We employ molecular modeling for analyzing the effect of post-translational phosphorylation on the structure of the catalytic domain of PrkC as the enzyme activity was shown to be regulated by multiple site phosphorylation, namely in the activation loop and additional phosphorylation site on large lobe of the kinase domain [26] (Fig. 2).

We carried out 5 ns long molecular dynamics (MD) simulations of phosphorylated and unphosphorylated forms of the PrkC catalytic domain (PrkCc) with and without its bio-ligand, adenosine triphosphate (ATP). We compare the phosphorylated and unphosphorylated structures of the

PrkCc to investigate the conformational changes of the activation segment. We also analyze the influence of the PrkC natural ligand, ATP, on the structural changes of the kinase catalytic domain.

Results and discussion

Sequence alignment

As more and more protein kinase structures were known, it became a fact that the function of the activation segment plays an important role in the regulation of the activity of most kinases [27]. Many of these enzymes are regulated by phosphorylation in the activation loop. Similarly, the PrkC activity is regulated by phosphorylation of the four threonine residues placed on the activation loop in positions: T162, T163, T165, T167 and one serine residue (S214) from the C-terminal lobe [26].

The sequence alignment between the PrkC and the PknB, *Mycobacterium tuberculosis* kinase, shows surprisingly high similarities, namely the 44.7% residue identity for 273 residues. The sequence alignment is presented in Fig. 3. Functional similarities between the PrkC and the PknB can be found in the literature [28–30]. We also focused on the alignment of the activation loop (see Fig. 4) of the PrkC to some other kinases from *Mycobacterium tuberculosis* (namely PknB, PknF, PknD, PknE). Both N- and C-terminal fragments are conserved. Only two threonine residues (T165, T167), important for kinase activity, out of four present in the PrkC molecule (indicated by arrows) were identified in *Mycobacterium* kinase. It was reported, that the mutation of these two threonine residues (T171, T173) in the PknB kinase as well as in the PrkC, result in a significant decrease of activity [30].

The serine residue in the position 214 is also very important for the activity of the enzyme [26]. When it was mutated to an alanine residue, activity reduced to 20% of the wild type (WT). There is no evidence that shows how this single residue can play such an important role. An equivalent residue was found in the PknB kinase (see Fig. 3) in the position 220 (PknB numbering), but it was not reported as important for the enzyme activity [31]. Based on the position on the surface of the enzyme, we speculate that its role could be meaningful for dimerization of the PrkC catalytic domains. It most likely creates contact with another residue from the dimer interface. This hypothesis will be verified in our future studies concerning the dimerization of the PrkCc.

ATP binding pocket

To analyze whether phosphorylation of the activation loop has an influence on the surrounding of the ATP we checked which residues are within 4.0 Å distance from the nucleotide in both complexes: PrkCc-ATP and pPrkCc-ATP. The results are presented in Fig. 5 and Table 1**.** We found 24 residues which occurred in contact with the nucleotide in the unphosphorylated complex. Only three residues out of twenty-four were missing in the pPrkCc-ATP complex. Over 87% of these residues were found as conserved ATP binding in other kinases by Vulpetti and Bossotti [32]. These results suggest that phosphorylation does not significantly influence the surrounding of ATP and indirectly confirms that the nucleotide was properly docked to its binding pocket.

As we were interested if the phosphorylation influence the shape of the nucleotide- binding pocket, we visualized models of PrkCc and pPrkCc and compared the space which is commonly known (See Fig. 6) to bind ATP. Strikingly, we observed that in the case of the phosphorylated model the ATP-binding cleft was deeper (side view in Fig. 6) and more accessible (front view in Fig. 6) than in the case of the unphosphorylated model (PrkCc). To check if the visualized ATP-binding cleft provides more surface for binding ATP, the Solvent-Accessible Surface (SAS) was calculated in VEGA [33]. Calculations of the SAS confirmed the observations. SAS for the PrkCc = 13256.4 Å and for the pPrkCc = 13740.9 Å. From those results we conclude that phosphorylation influence the conformational changes of the PrkCc and enlarge the surface accessible for binding the ATP.

Conformational diversity of the activation segment

We investigate here the structural changes of the activation segment in the PrkCc models. To visualize this, we overlaid 10 structures (so called "snapshots") of the MD production run, they consisted of the 10 complete sets of coordinates saved after every 500 ps, beginning from 500 to 5,000 ps (Fig. 7). We observed, that in non-phosphorylated model (PrkCc, Fig. 7a) as well as the phosphorylated and complexed with ATP model (pPrkCc-ATP, Fig. 7d), conformation of the activation segments remained stable, inactive and active state, respectively. On the other hand, the activation fragment shows high conformational flexibility, in both models: the PrkCc-ATP (Fig. 7b) and in the pPrkCc (Fig. 7c). These results suggest that the phosphorylation of the activation loop or binding the ATP molecule induce conformational changes of the activation segment, however, a separated event (binding ATP or phosphorylation) can not force complete shift from an inactive to active state.

For better understanding of the structural plasticity of the activation segment, we indicated two C^{α} atoms of residues (G154, T167) which are important for activation of the enzyme (see Fig. 7). The glycine residue, which is a

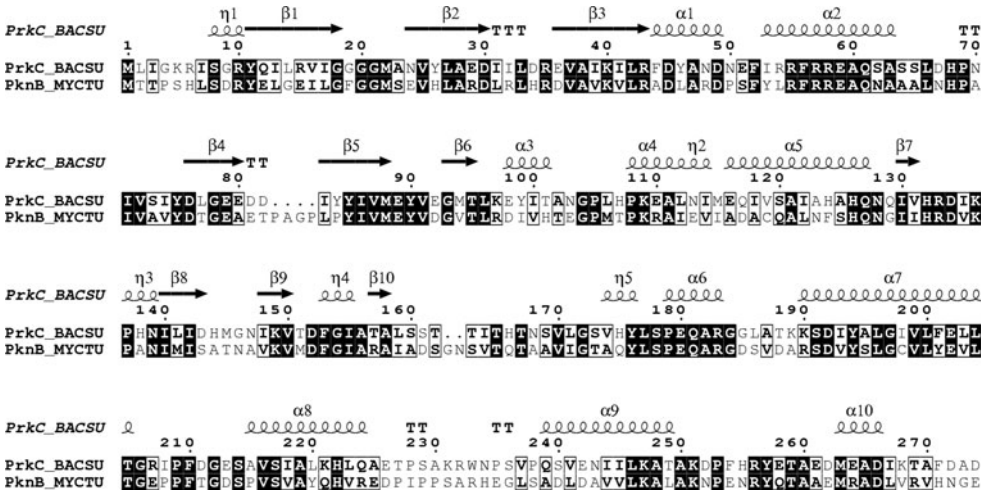

Fig. 3 The catalytic domain of *Bacillus subtilis* PrkC kinase aligned with a fragment of *Mycobacterium tuberculosis* PknB kinase. The alignment was done using ESPript 2.2 program

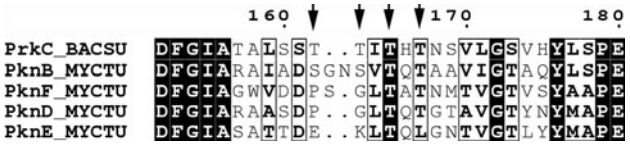

Fig. 4 The alignment of the activation loops of PrkC, PknB, PknF, PknD, PknE. The PrkC threonine residues which regulate the activity of the enzyme are indicated by *arrows*

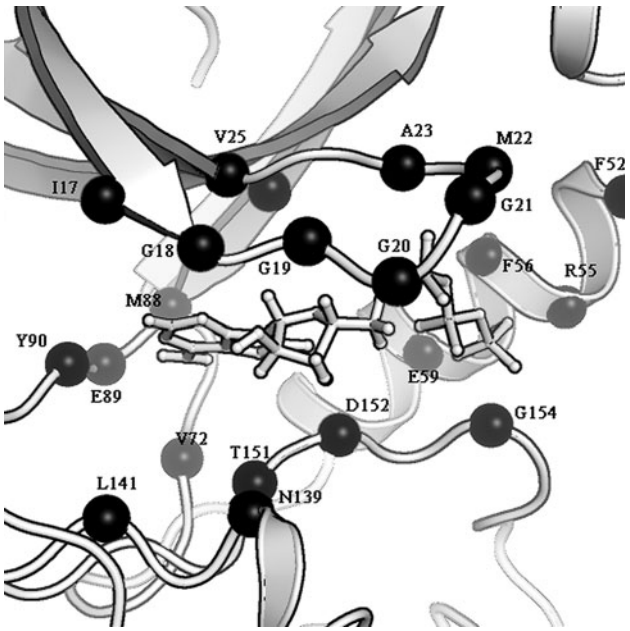

Fig. 5 ATP binding pocket. Residues closer than 4.0 Å are presented as spheres in the position of Cα atoms. ATP is presented as sticks and PrkCc interface as cartoon representation

Table 1 Percentage occurrences of residues from ATP binding region calculated by Vulpetti and Bosotti [32]

Residue	Pos. in CDK2	PrkCc-ATP	pPrkCc-ATP	Perc*
I17	10	+	+	37
G18	11	+	+	94.8
G19	12	+	+	1.9
G20	13	+	+	99.1
G21	14	+	+	10.4
M22	15	+	+	67.3
A23	16	+	+	11.4
V25	18	+	+	95.5
A38	31	+	−	94.8
K40	33	+	+	97.6
F52	None	+	+	n.a.
R55	None	+	+	n.a.
F56	None	+	−	n.a.
E59	51	+	+	96.4
V72	64	+	+	56.6
M88	80	+	+	40
E89	81	+	+	78
Y90	82	+	+	43.6
K136	129	+	−	76.3
N139	132	+	+	98.6
L141	134	+	+	80.8
T151	144	+	+	15.9
D152	145	+	+	98.8
G154	147	+	+	97.6

* Percentage occurrences of residues from ATP binding region calculated by Vulpetti and Bosotti

part of the DFG-motif (Asp-Phe-Gly), is conserved in serine-threonine kinases and it is placed at the N-terminus of the activation fragment. In the active state, the DFG-motif typically forms a polar contact with ATP phosphates, either directly or via magnesium cation [19]. In some kinases the structural changes that originate from the activation loop are translated into distortions of the DFG motif. The position of the glycine from the DFG motif in the pPrkCc-ATP model is different than in the PrkCc, PrkCc-ATP models. In the pPrkCc-ATP model, the C^{α}

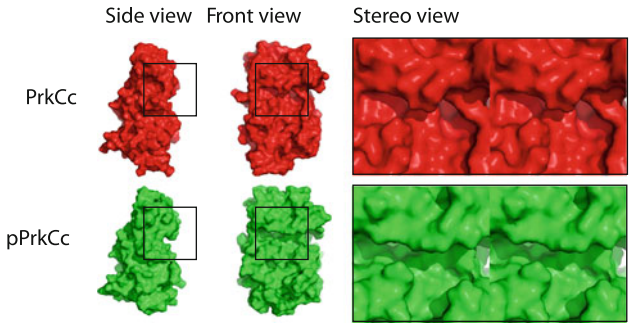

Fig. 6 Surface visualization of models: PrkCc (*red*) and pPrkCc (*green*) with the ATP-binding pocked (*black frame*)

atom of G154 residue is positioned horizontally and in the model of pPrkCc it is switching between position vertical and horizontal. The second residue, indicated in the Fig. 7 is T167. Position of the C^{α} atom changes in two models: PrkCc-ATP (*panel b*) and pPrkCc (*panel c*). Mechanism of this conformational plasticity is different. In model PrkCc-ATP, the loop is simply unstable and the conformation of the residue flips back and forth. The model of the phosphorylated (pPrkCc) activation loop shows rather translational movement, towards the helix above (αC-helix), which changes the shape of the loop. In the sections below, we describe interactions that influence the changes in greater detail.

To get a better view on the conformational diversity-effect in the PrkCc model, the RMSd was calculated for the activation loop (see Fig. 8) and for the DFG-motif (see Fig. 9). RMSd amplitude was used as a measure of the structural plasticity. Consequently with the results above, the most stable conformation of the activation loop was found in the pPrkCc-ATP model. Our calculations also confirmed instability of the loop in the PrkCc-ATP, as well as structural changes in the pPrkCc model. The DFG-motif presents the highest instability of its conformation in the PrkCc-ATP model during whole time of the analysis. In the pPrkCc-ATP model, the DFG motif was the most stable. It is also worth noting, that the conformation of the DFG motif in phosphorylated PrkCc (pPrkCc) model was mostly stable during the first 3 ns and then started switching. It was observed to be the result of the translational movement of the activation loop (see Fig. 7) between 2.5 and 3.0 ns (Fig. 8), when the RMSd changes from 1.5 to 2.5 Å.

To gain more information about conformational changes of the activation loop we also calculated the Root Mean Square fluctuation, which shows movement of residues in the time of the simulation. Figure 10 confirms the stability of the loop in two models: PrkCc and pPrkCc-ATP. What also stands out is the large value of RMSf of threonine in the position 167 in PrkCc-ATP. It is clear that instability of this residue effects the conformation of the activation loop

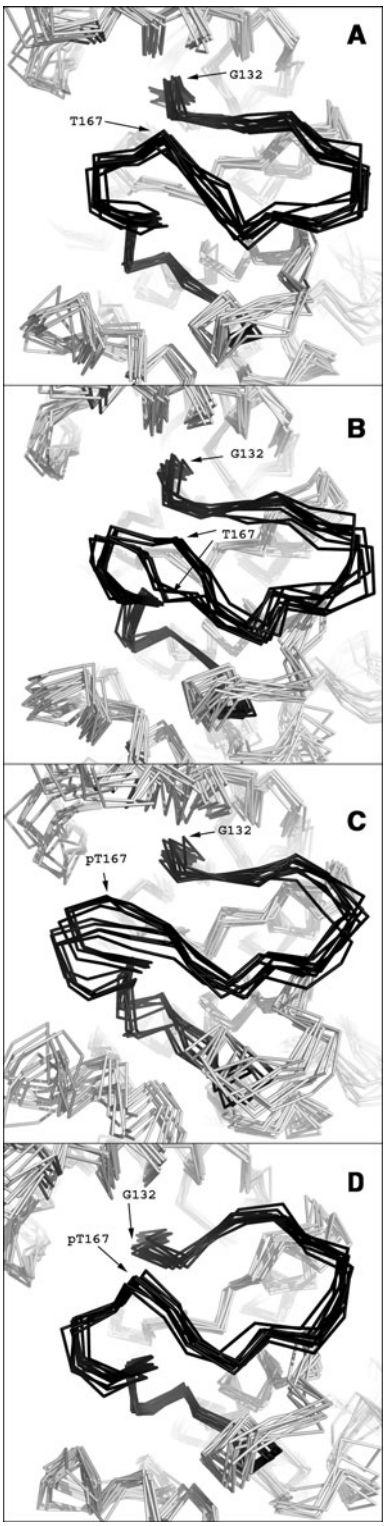

Fig. 7 The superposition of the activation segments of the PrkCc models

(see Fig. 7b). The value of the RMSf for the same residue in the phosphorylated model (pPrkCc) is also higher than the values in the rest of the models (PrkCc and

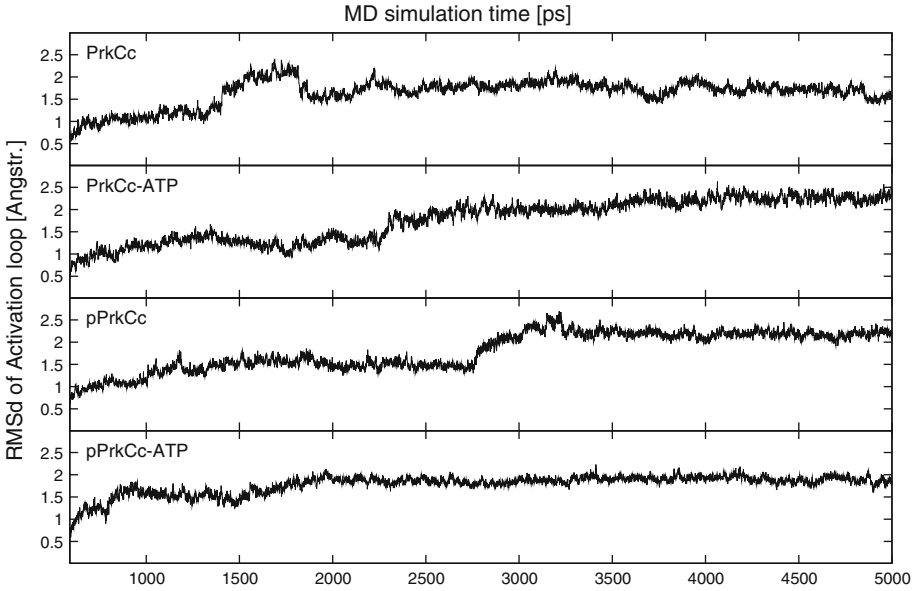

Fig. 8 The RMSd plot of the activation loop for different states of its loop phosphorylation and ATP-binding

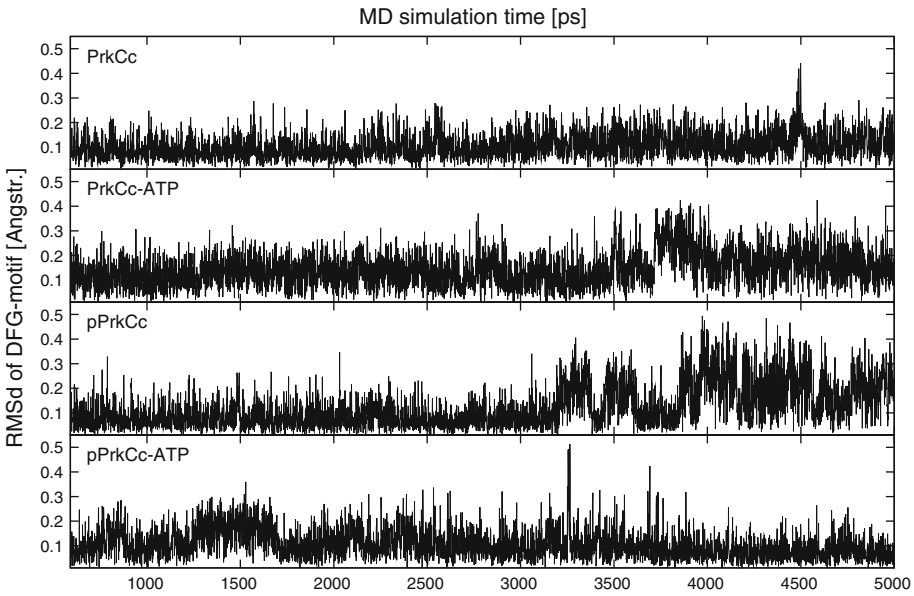

Fig. 9 The RMSd as a function of time, calculated for DFG-motif

pPrkCc-ATP), but only reflects the translational movement shown in *panel c* of Fig. 7.

Summarizing these results, we conclude that the binding of the nucleotide to an unphosphorylated model of the kinase induced the instability in the DFG-motif and the activation loop. Phosphorylation stabilized the activation loop and stimulated some conformational changes in the DFG-motif. Both ATP-binding and the phosphorylation of the activation loop are obligatory factors for the stabilization of the activation loop and in the consequence, the whole activation segment.

This data shows strict correlation in the molecular mechanism between two catalytically important fragments, the activation loop and the DFG-motif. Furthermore, we ask the question, "How are conformational changes induced by phosphorylation or binding the nucleotide important for the enzyme activity?" In the next section we try to answer this question by analyzing three conservative motifs that are well known to be important for the activity of the kinases.

Active or inactive conformation

DFG-motif

In many kinases the conformational change of the DFG-motif ("DFG flip") correlates with the activity of the enzymes. This structure–function dependence has been

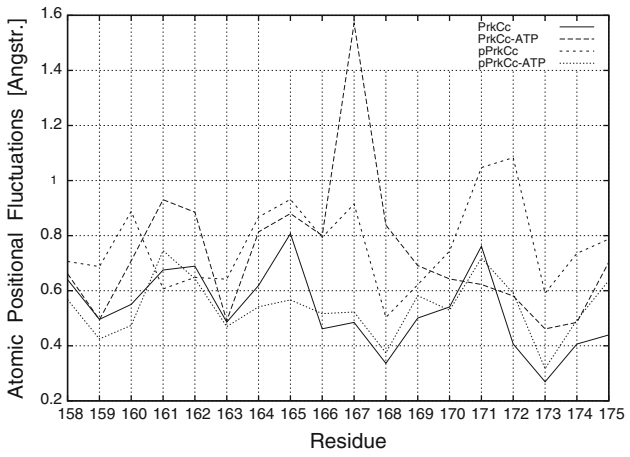

Fig. 10 Visualization of the RMSf calculations for the activation loop

widely studied [19, 32, 34–38] but still remains unclear. The conserved aspartate from the DFG motif is known to chelate a magnesium cation which positions the phosphates of the nucleotide [34, 39, 40]. This position is called "DFG-in" and is observed in the active form.

In the case of PrkCc models we observe two different conformations. The first conformation was observed in PrkCc and pPrkCc and is characterized as "DFG-out" (Fig. 11a and c, respectively) [41, 42]. The D152 residue removes its sidechain from the position in which it coordinates the Mg^{2+} ion. The second conformation is observed only in the presence of ATP, namely models PrkCc-ATP and pPrkCc-ATP and is called DFG-in (see Fig. 11b and d, respectively). The second difference between these

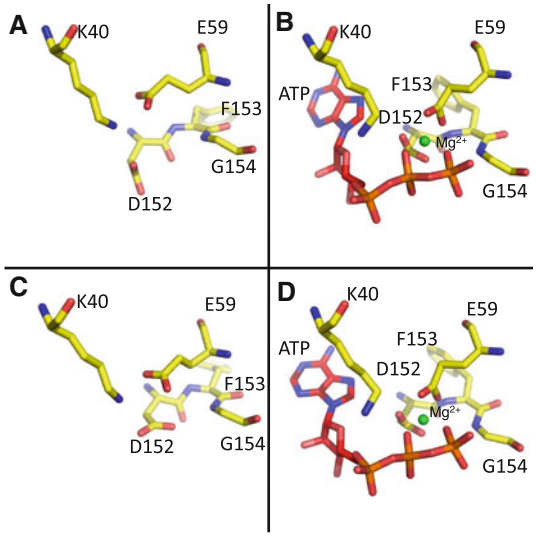

Fig. 11 DFG-motif presented in the "out" for **a** and **c** (respectively PrkCc, pPrkCc) and "in" for **b** and **d** (respectively, PrkCc-ATP, pPrkCc-ATP) conformation

conformations is the position of phenylalanine (F153). In the absence of the nucleotide, the F153 points down to αE-helix and in the presence of the ATP is pointed toward the V72, which are conserved residues forming the ATP pocket (see Table 1). We speculate that F153 can create a hydrophobic interaction with the V72, since the distance between those residues is about 2.3 Å (data not shown). Consequently, this interaction shields the adenine from solvent molecules increasing a so-called "buried region" [32]. The role of G154 remains undefined. Kornev et al. [19] suggested that the hydrogen bond between N–H of glycine and negatively charged oxygen of the aspartate stabilizes the conformation of the aspartate. Disruption of this hydrogen bond can loosen the magnesium-binding loop providing a possibility for the "DFG-flip". To verify this thesis in the case of PrkCc, we measured the distances between the carboxylate group of D147 and hydrogen atom of G149 during our 5 ns MD simulations. Again, when the ATP was present in the complexes, the distance was about 3.1–3.2 Å and without the presence of ATP molecule the distance was about 3.6–4.4 Å (data not shown). The distances measured during MD simulations cannot be considered with forming a hydrogen bond as they are too long, but may still be a reflection of an interaction which might stabilize the position of the aspartate residue in its active state.

αC-helix

We were also interested in the conformation of the αC-helix where another conservative residue is found, namely E59. When αC-helix is displaced or rotated from the active site this conformation is called "αC-out" and characteristic for inactive state [13, 43–45]. In contrast, when the helix is properly located with glutamate residue placed toward the ATP binding pocket, the conformation is called "αC-in," characteristic for an active state [19, 37, 38]. In the αC-in conformation, a characteristic ionic bond is found between conserved glutamate residue (E59) [46] and lysine (K40 in the PrkCc) from the *β*3-strand (see Fig. 11). Distance between the amino group of K40 and the carboxylate group of E59 was examined during MD simulations for our models and showed a remarkable result. We found a relationship between the presence of ATP and αC-in/αC-out conformation. For complexes which possessed the nucleotide, the measured distance was about 5 Å and for those without ATP, the residues were closer (3–3.5 Å). This is caused by creating new interactions: negatively charged glutamate residue coordinate positively charged Mg^{2+} ion. On the other hand, the positively charged lysine residue starts to interact with negatively charged phosphates of the ATP. It is worth noting that lysine 40 is closer to glutamate 59 in the phosphorylated model (pPrkCc) than

unphosphorylated (PrkCc). This will be explained in the Sect. "Activation loop interacts with the αC-helix".

HRD-motif

For further studies of active conformation of phosphorylated models of PrkC catalytic domain we examined the conserved HRD triad (residues 132–134, see Fig. 3). First, we considered the spatial arrangement of the arginine residue (R133). It is known that in the active conformation it interacts with the phosphate residue from the activation loop [17, 37]. In the case of the phosphorylated PrkCc model, it interacted with a phosphorylated threonine residue in position 163 (pT163, see Fig. 12c and d). When the threonine residue was not phosphorylated we found hydrogen bonds between the oxygen atom present in hydroxyl group of the threonine 163 and hydrogen atoms from a guanidinium group of the arginine 133 (Fig. 12a). We did not find these contacts in the PrkCc-ATP model, since the arginine 163 was not positioned toward the activation loop (Fig. 12b). Secondly, we observed the position of the following invariant residue, aspartate in the position 134, involved in the catalytic mechanism [27, 47]. In all of our models this residue (D134) forms the salt-bridge interaction with the nearby lysine side-chain residue in the position 136 (Fig. 12). Only the PrkCc model displays additional interaction of the aspartate residue with S173 from the P + 1 [48] loop. These results confirm the role in the catalytic mechanism of the aspartate residue which may activate the hydroxyl group of the incoming substrate [17]. Both residues, the D134 and the K136, are highly conserved in Ser/Thr Protein Kinases [49] and can also be involved in the electrostatic stabilization of the transition state because of the charged groups at the end of their side chain as suggested by Madhusudan et al. [50].

Activation loop interacts with the αC-helix

Through analyzing the structure of PrkCc models, we found an ionic interaction between two of the phosphorylated threonine residues (pT165 and pT167) with the use of magnesium ion (see Fig. 12c and d). This interaction may be crucial for interactions found between pT167 and the positively charged arginine cluster (R54, R55 and R58) which is present in the αC-helix (see Fig. 13c). We assume that it is the residue in positions T165 and T167 in the direction of αC-helix. Our hypothesis, based on the calculations correlate with biological experiments [26], namely mutagenesis of both T165A and T167A, which shows meaningful decrease of the enzyme activity from 100% in WT to ∼4% in the case of the mutant.

These interactions can be interpreted as salt bridges and convincingly, may have an impact on the proper position of the phosphate binding site, namely residue E59. This mechanism, consisting of a basic residue from αC-helix interacting with phosphorylated residue from the activation loop, was also seen in other kinases: active MAPK kinase (residue equivalents R68-pT183), PKB (H196-pT309) [35]. These interactions provide a link between N-terminal and C-terminal lobes of the kinase [27] and may stabilize the active (closed) conformation. We did not find any other motions that would confirm the role of the phosphorylation in the catalytic domain closure. This may provide evidence as these interactions may play a role in the proper orientation of the catalytic residue E59. Another function of these interactions would be the recognition of peptide substrate, as it is in the case of cAPK [51]. It is also known that the PrkC forms a dimer. The interactions between arginine residues, cluster from the helix, and phosphorylated threonine residue might mediate the enhancement in dimerization affinity, as it was postulated by Cole [52] in the case of the PKR kinase. We suggest mutagenesis of the charged arginine residues R54, R55 and R58 to test this hypothesis.

Furthermore, a popular mechanism of rotation of the αC-helix [19] maintains latency, because of other salt-bridge interaction between R57 and E79 placed in the β4-sheet of the PrkCc. These contacts were found in the phosphorylated model, but predominate in the pPrkCc-ATP model (see Fig. 13), which means that the presence of the nucleotide, as well as the phosphorylation process, plays an important role of the αC-helix position stabilization.

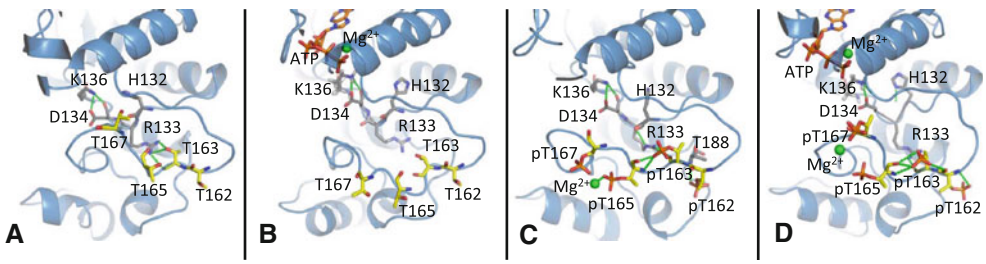

Fig. 12 HRD-motif (residues 132–134) and phosphorylated threonine interaction network

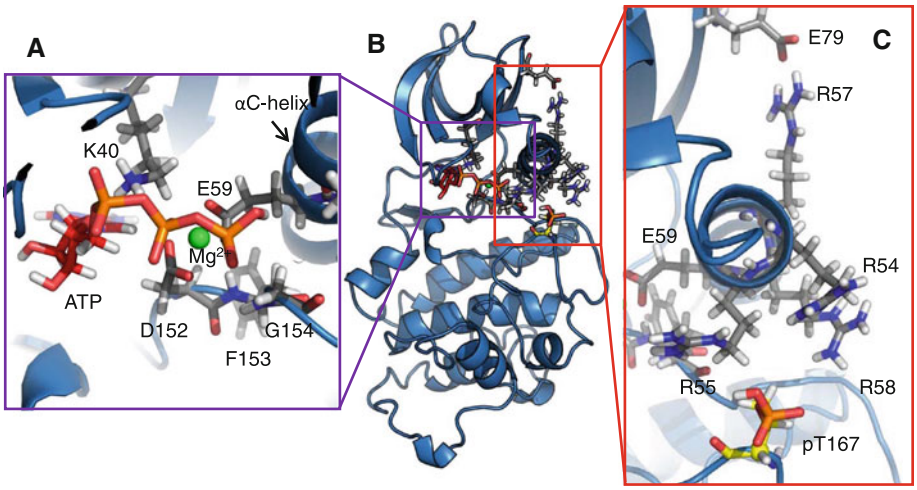

Fig. 13 Active state, closed conformation of the pPrkCc-ATP complex **a** DFG-in, αC-in position, **b** The pPrkCc-ATP complex, **c** Strong salt bridge interactions of the αC-helix

ATP binds after phosphorylation

Based on the results presented above, we hypothesize that binding of an ATP molecule into the nucleotide-binding pocket takes place after the phosphorylation of the activation loop, and it is probably less effective without this process.

Instability of conformation of the activation loop in PrkCc-ATP complex may have biological significance. In the dormant spores, ATP is the limiting factor. Instability of conformation of the DFG-motif, observed throughout all time of the simulation, may be a consequence of binding ATP to the inactive form (unphosphorylated) of the kinase and may increase the pool of remaining nucleotides to be used by the active PrkCc molecule. The synthesis of ATP starts during outgrowth long after the action of PrkC as a germination receptor described by Shah and co-workers [22]. Taking all of this into account, it is very important for the spore to reduce usage of ATP by non- or not fully phosphorylated PrkC molecules by reduction of stability of such complexes. Visualization of the surface of PrkCc and pPrkCc, as well as, solvent-accessible surface calculations for those models also indicates as the ATP binds to the phosphorylated model of PrkCc, rather than unphosphorylated.

The pPrkCc model seems to be an intermediate state, between the unphosphorylated PrkCc and pPrkCc-ATP. This hypothesis is based on our results and can be also observed on the molecular level, analyzing one of the most important for the enzyme activity structural motif, the DFG-triad. Instability of the motif was only observed in the PrkCc-ATP model; although it showed that presence of the nucleotide induce active state ("αC-in" and "DFG-in"). When the ATP is bound, the D152 (part of the DFG-motif) creates ion binding with the magnesium cation, nearest to the phosphates of the ATP (see Figs. 11d and 13a). This interaction was also found by Adams et al. in 2001 [34]. In the case of the PrkCc-ATP model this interaction is similar (Fig. 11b), although we discovered the additional close contact between the R55, to the αC-helix and oxygen atom of the G154 (also from the DFG motif) which destabilize the DFG-motif. In the pPrkCc-ATP model, the R55 creates rather stronger ion interaction with the negatively charged phosphorylated residue of T167 (showed in Fig. 13c) than with the G154 as it was in the case of the PrkCc-ATP model. What is more interesting, is that the "DFG-flip" was observed in the phosphorylated model (pPrkCc, see Fig. 7c), from the inactive position found in PrkCc (Fig. 7a) to the active position found in the pPrkCc-ATP (Fig. 7d).

Conclusion

Comparative molecular dynamics simulations of four complexes: PrkCc, PrkCc-ATP, pPrkCc and pPrkCc-ATP have been performed. The sequence alignment of the PrkC showed high similarities in catalytic domain as well as the activation loop with the PknB kinase from *Mycobacterium tuberculosis*. Analysis of the ATP binding pocket, within phosphorylated and unphosphorylated complex, did not affect nucleotide contact residues, which were highly conservative.

Three structural fragments, characteristic for the activity of the enzyme, were studied: DFG-motif, HRD-motif and αC-helix. It was shown that the presence of ATP is responsible for most of their spatial changes. DFG-in conformation was seen only when the nucleotide was placed in the binding pocket. The αC-helix position was found stable, as the strong salt-bridge interactions were present. The overall position of the HRD triad stays the same for most of the models (besides PrkCc-ATP) and confirms the active state of the enzyme.

Studies on the phosphorylated residues brought some ideas about their role. The phosphorylation loop, by its

interactions with positively charged arginine cluster and found in αC-helix, stabilizes the position of the catalytically important residue E59. We confirmed that its function does play a critical role in the conformational changes of the kinase, such as increasing the nucleotide-binding pocket. It is also probably involved in the substrate recognition or dimerization and likewise for the phosphorylated threonine (pT162) and serine (pS214) residues. Their position on the surface of the enzyme strongly suggests a role in the dimerization capability.

Based on our study we find phosphorylated catalytic domain of the PrkC, complexed with ATP (pPrkCc-ATP), as a fully active conformation in the closed position. Results reported in this paper brought us to the hypothesis that the ATP binds after phosphorylation of the activation loop and not before. This hypothesis will be verified shortly in a biochemical experiment.

We firmly believe that this work shows significance of using the molecular modeling tools in investigation of the structure–function relationship in protein kinases which activity is influenced by post-translational modification. Methodology used here can be widely utilized by researchers wishing to have more insight into enzyme activity on the molecular level/and other QSAR studies.

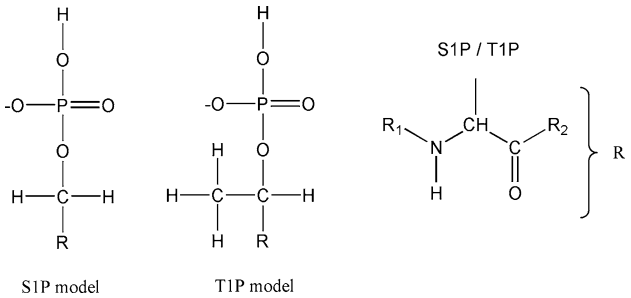

Fig. 14 The structure of phosphorylated serine (S1P) and threonine (T1P) residues

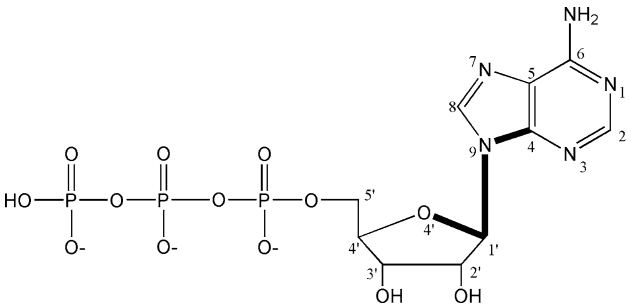

Fig. 15 The structure of the ATP3- model

Methods

Modeled structures

Since the experimental, three-dimensional structure of the PrkC kinase is still unknown, the initial arrangement of the PrkC catalytic domain was built based on the SWISS-MODEL [53] suggestions, using known crystallographic structures of Hanks kinases as a template. The initial structure of the PrkCc was optimized in AMBER 8.0 force field [54]. Detailed procedure about construction of the PrkCc model is described in our previous work [55].

The PrkCc model with phosphorylated residues T162, T163, T165, T167, S214 (called by us the phosphorylated PrkCc) was built using XLEAP, module of AMBER 8.0 package [56]. The parameters of phosphorylated serine (S1P) and threonine (T1P) residues used here were previously published by Homeyer et al. [57]. Models of S1P and T1P are presented in Fig. 14. The conditions found in the spores, especially the low value of pH [24] influence the charge of amino acid residues containing titrable groups. Based on the pKa values of phosphothreonine and phosphoserine (~6.5 both [58]) we used single negatively charged models (S1P and T1P) of the phosphorylated residues.

The ATP model was built based on Cambridge Structural Database (entry ADENTP03 [59]) and modified, to take into account the negative charge of ATP^{3-}, (shown in Fig. 15) using MOLDEN [60]. Calculations of the electrostatic potential of ATP were carried out using the ab initio method implemented in program GAMESS [61] at the HF/6-31G* level. The partial atomic charges were determined based on the electrostatic potential using the restrained electrostatic potential (RESP) procedure [62]. In Table 2 we present the internal coordinates of ligand arranged in the Z-Matrix form with partial atomic charges included. Table 3 includes modifications introduced by us into the parameters prepared by Carlson et al. [63] which apply to the ATP molecule.

Docking ATP into the PrkCc

In our previous work [55] we compared the 38-residue fragment responsible for binding the ATP [32] with PrkCc modeled structure. Thirty out of 38 residues were conserved indicating that the ATP binding cleft is placed within the catalytic domain of PrkC between the small and the large lobes. A box delimiting ATP was built inside the PrkCc that contained all of the 30 conserved residues. ATP was docked inside the phosphorylated and unphosphorylated model of the PrkCc with the AUTODOCK 3.0 program [64] using the GENETIC ALGORITHM procedure [65].

The docking procedure generated 4 sets of 30 complexes, both for phosphorylated and unphosphorylated

Table 2 Internal coordinates of ligand arranged in the Z-Matrix form with partial atomic charges

AMBER atom type	Bond		Angle		Dihedral	charge	
H							0,464
OH	1	0,950					−0,538
P	2	1,417	1	109,466			1,024
O2	3	1,443	2	127,156	1	60,188	−0,759
O2	3	1,378	2	116,414	1	−77,043	−0,840
OS	3	1,742	2	105,152	1	−179,995	−0,371
P	6	1,511	3	135,440	4	128,516	1,032
O2	7	1,413	6	113,606	3	−28,938	−0,719
O2	7	1,618	6	103,890	3	−164,747	−0,881
OS	7	1,733	6	96,250	3	83,536	−0,374
P	10	1,516	7	131,604	8	−10,192	1,079
O2	11	1,525	10	115,350	7	−92,994	−0,828
O2	11	1,409	10	109,230	7	53,771	−0,761
OS	11	1,749	10	97,292	7	164,275	−0,387
CT	14	1,428	11	117,322	13	176,867	−0,164
H1	15	1,088	14	119,887	11	−9,976	0,053
H1	15	1,089	14	129,696	11	87,717	0,149
CT	15	1,445	14	107,841	11	−136,050	0,417
H1	18	1,089	15	110,146	14	−146,856	0,015
OS	18	1,576	15	105,191	14	−48,012	−0,433
CT	20	1,562	18	99,296	15	148,231	0,000
H2	21	1,089	20	102,535	18	106,676	0,103
N*	21	1,650	20	99,659	18	−129,450	−0,160
CK	23	1,399	21	121,707	20	−51,671	0,081
H5	24	1,088	23	118,122	21	4,395	0,199
NB	24	1,326	23	111,838	21	−177,470	−0,517
CB	26	1,364	24	104,651	23	2,150	−0,029
CA	27	1,447	26	131,868	24	−176,984	0,647
N2	28	1,439	27	123,753	26	−3,494	−0,931
H	29	1,008	28	120,000	27	179,994	0,386
H	29	1,008	28	120,000	27	−0,003	0,396
NC	28	1,363	27	114,721	26	173,498	−0,715
CQ	32	1,369	28	122,816	27	4,916	0,381
H5	33	1,088	32	124,906	28	175,495	0,097
NC	33	1,310	32	125,613	28	−5,665	−0,631
CB	27	1,403	28	115,591	32	−0,429	0,529
CT	18	1,538	20	102,684	21	21,596	0,009
H1	37	1,089	18	110,032	20	79,166	0,189
OH	37	1,390	18	114,134	20	−157,678	−0,696
HO	39	0,949	37	109,472	18	−179,996	0,424
CT	21	1,396	23	121,304	36	−0,007	0,290
H1	41	1,088	21	109,471	23	−32,259	0,024
OH	41	1,368	21	108,901	23	−152,264	−0,672
HO	43	0,950	41	109,471	21	179,996	0,423

PrkCc models. All complexes were examined using XLEAP, module of the AMBER 8.0 package [56], to find possible structural abnormalities by measuring distances between atoms and also with RASMOL [66] to inspect structures and verify the possible existence of any clashes between atoms. The structures of all complexes were optimized using SANDER, module of the AMBER 8.0 package, in a vacuum and once more, after immersing in explicit water model (TIP3P).

Table 3 Modifications introduced into the parameters prepared by Carlson et al. [63] which apply to the ATP molecule

Bond	Parameters			
H–OH	553.	0.960		
Angle	Parameters			
H–OH–P	45.0	108.500		
Dihedral	Parameters			
H–OH–P–OS	3	20.75	180.0	3.
NB–CB–CB–NC	4	21.80	180.0	2.
CA–CB–NB–CK	2	5.10	180.0	2.

To extract the correct structures we decided to measure the torsion angle (χ), defined by atoms C4-N9-C1'-O4' (presented as thick bonds in Fig. 15) of ATP molecule and chose only the anti conformation [66]. This choice was thoroughly documented in [55]. The other criterion taken into consideration was the proper arrangement of the ATP within its binding pocket. It was compared to the most resembling the PrkC molecule kinases, known from crystallographic studies (PDB codes as follows: 2ACX, 1CDK, CDK2). Out of all complexes fulfilling both criteria, we chose one for each phosphorylated and unphosphorylated model with the lowest energy value for further Molecular Dynamics (MD) simulations.

Molecular dynamics simulations

The Molecular dynamics simulations of phosphorylated and unphosphorylated PrkCc models (presented in Fig. 2) with and without ATP were carried out for 5 ns, with the use of AMBER 8.0 [56]. The heating stage lasted for 250 ps and afterwards, during the MD production run, the temperature stabilized at 280 K (the same as in our previous work). All calculations were carried out with constant pressure MD with anisotropic pressure scaling. The non-bonded cutoff distance was 10 Å. Bonds involving hydrogen atoms were constrained using the SHAKE algorithm [67, 68]. Temperature scaling using the Berendsen coupling algorithm [69] was applied during all MD runs.

To analyze if phosphorylation of the activation loop has an influence on the surrounding of the ATP we checked which residues are within 4.0 Å distance from the nucleotide in both complexes: PrkCc-ATP and pPrkCc-ATP. This was made by calculating the distances during the time

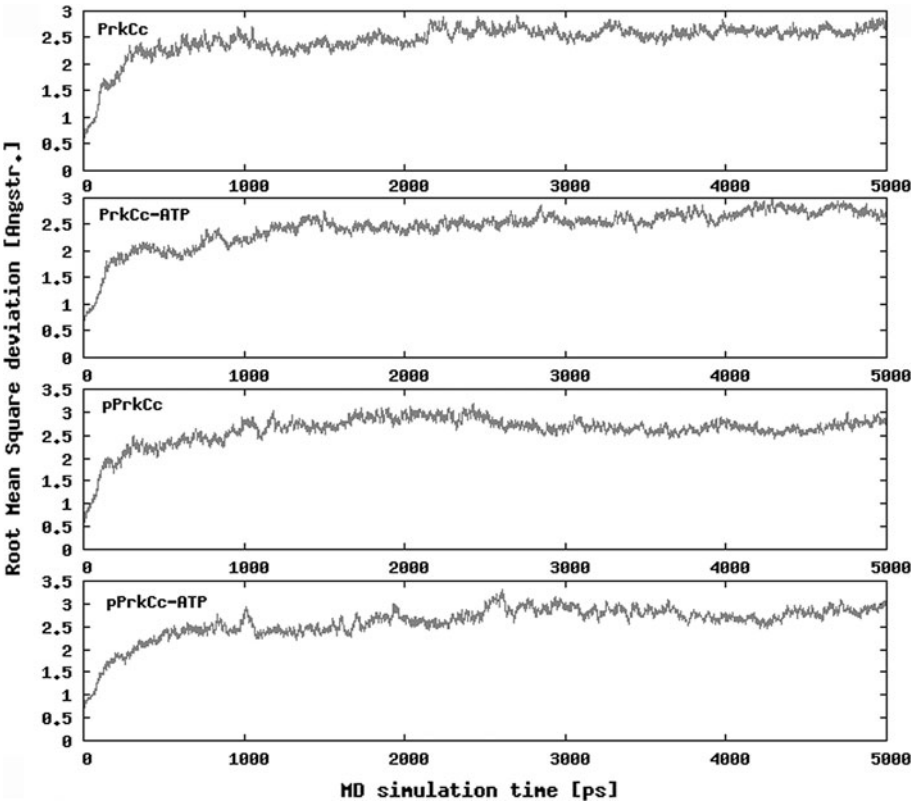

Fig. 16 The plots of time dependent RMSd over all atoms of the PrkCc models during 5 ns MD simulations

of the simulation using PTRAJ, an AMBER 8.0 [56] module.

The Root Mean Square deviation (RMSd) was calculated after the stabilization time (starting from 500 ps), and its amplitude was used as a measure of structural stability. The first structure after the stabilization time was used as a reference. All atoms present in single PDB file, recorded after every 1 ps, were compared to the initial structure. The results presented in Fig. 16 show that each trajectory is stable after 500 ps. RMSf calculations were made for all of C^{α} atoms after the stabilization time ($t = 500$ ps) for each of the models of PrkCc.

The visualization of the models from the Molecular Dynamics simulation was made with use of PyMOL [70].

Computer equipment

All calculations were carried out on a small cluster of computers placed in Faculty of Chemistry, University of Gdansk. The cluster is of a heterogeneous nature and it consists of:

- 4 nodes with 2 processors AMD DualCore Opteron 270 2 GHz 2 GB RAM
- 14 nodes with processor Intel QuadCore Q6600 2.4 GHz 4 GB RAM
- 12 nodes with processor Intel QuadCore Q9400 2.6 GHz 8 GB RAM
- 16 nodes with processor AMD Sempron 2800 + 2 GHz 1 GB RAM
- 6 nodes with processor AMD Athlon64 2800 + 1.8 GHz 0.5 GB RAM
- 4 nodes with processor AMD Athlon XP 1800 + 1.5 GHz 0.5 GB RAM
- 3 nodes with processor AMD Athlon 1 GHz 1 GB RAM

Each of the protein/complex systems was calculated using the average CPU time of 650 h.

Acknowledgments We acknowledge Tiffany S. Han for critical reading of the manuscript. This work was partially supported by University of Gdańsk fund DS/B50A-4-162-8.

References

1. Rubin GM, Yandell MD, Wortman JR, Gabor Miklos GL, Nelson CR, Hariharan IK, Fortini ME, Li PW, Apweiler R, Fleischmann W, Cherry JM, Henikoff S, Skupski MP, Misra S, Ashburner M, Birney E, Boguski MS, Brody T, Brokstein P, Celniker SE, Chervitz SA, Coates D, Cravchik A, Gabrielian A, Galle RF, Gelbart WM, George RA, Goldstein LS, Gong F, Guan P, Harris NL, Hay BA, Hoskins RA, Li J, Li Z, Hynes RO, Jones SJ, Kuehl PM, Lemaitre B, Littleton JT, Morrison DK, Mungall C, O'Farrell PH, Pickeral OK, Shue C, Vosshall LB, Zhang J, Zhao Q, Zheng XH and Lewis S (2000) Comparative genomics of the eukaryotes. Science 287: 2204

2. Hakansson S, Galyov EE, Rosqvist R, Wolf-Watz H (1996) The Yersinia YpkA Ser/Thr kinase is translocated and subsequently targeted to the inner surface of the HeLa cell plasma membrane. Mol Microbiol 20:593
3. Hinc K, Nagorska K, Iwanicki A, Wegrzyn G, Seror SJ, Obuchowski M (2006) Expression of genes coding for GerA and GerK spore germination receptors is dependent on the protein phosphatase. PrpE J Bacteriol 188:4373
4. Madec E, Laszkiewicz A, Iwanicki A, Obuchowski M, Seror S (2002) Characterization of a membrane-linked Ser/Thr protein kinase in Bacillus subtilis, implicated in developmental processes. Mol Microbiol 46:571
5. Petrickova K, Petricek M (2003) Eukaryotic-type protein kinases in Streptomyces coelicolor: variations on a common theme. Microbiology 149:1609
6. Shi L, Potts M, Kennelly PJ (1998) The serine, threonine and/or tyrosine-specific protein kinases and protein phosphatases of prokaryotic organisms: a family portrait. FEMS Microbiol Rev 22:229
7. Iwanicki A, Herman-Antosiewicz A, Pierechod M, Seror SJ, Obuchowski M (2002) PrpE, a PPP protein phosphatase from Bacillus subtilis with unusual substrate specificity. Biochem J 366:929
8. Obuchowski M, Madec E, Delattre D, Boel G, Iwanicki A, Foulger D, Seror SJ (2000) Characterization of PrpC from Bacillus subtilis, a member of the PPM phosphatase family. J Bacteriol 182:5634
9. Vijay K, Brody MS, Fredlund E, Price CW (2000) A PP2C phosphatase containing a PAS domain is required to convey signals of energy stress to the sigmaB transcription factor of Bacillus subtilis. Mol Microbiol 35:180
10. Yudkin MD, Clarkson J (2005) Differential gene expression in genetically identical sister cells: the initiation of sporulation in Bacillus subtilis. Mol Microbiol 56:578
11. Mijakovic I, Poncet S, Boel G, Maze A, Gillet S, Jamet E, Decottignies P, Grangeasse C, Doublet P, Le Marechal P, Deutscher J (2003) Transmembrane modulator-dependent bacterial tyrosine kinase activates UDP-glucose dehydrogenases. EMBO J 22:4709
12. Knighton DR, Zheng JH, Ten Eyck LF, Ashford VA, Xuong NH, Taylor SS, Sowadski JM (1991) Crystal structure of the catalytic subunit of cyclic adenosine monophosphate-dependent protein kinase. Science 253:407
13. De Bondt HL, Rosenblatt J, Jancarik J, Jones HD, Morgan DO, Kim SH (1993) Crystal structure of cyclin-dependent kinase 2. Nature 363:595
14. Goldberg J, Nairn AC, Kuriyan J (1996) Structural basis for the autoinhibition of calcium/calmodulin-dependent protein kinase I. Cell 84:875
15. Hubbard SR, Wei L, Ellis L, Hendrickson WA (1994) Crystal structure of the tyrosine kinase domain of the human insulin receptor. Nature 372:746
16. Zhang F, Strand A, Robbins D, Cobb MH, Goldsmith EJ (1994) Atomic structure of the MAP kinase ERK2 at 2.3 A resolution. Nature 367:704
17. Johnson LN, Lewis RJ (2001) Structural basis for control by phosphorylation. Chem Rev 101:2209
18. Kannan N, Neuwald AF (2005) Did protein kinase regulatory mechanisms evolve through elaboration of a simple structural component? J Mol Biol 351:956
19. Kornev AP, Haste NM, Taylor SS, Eyck LF (2006) Surface comparison of active and inactive protein kinases identifies a conserved activation mechanism. Proc Natl Acad Sci USA 103:17783
20. Groban ES, Narayanan A, Jacobson MP (2006) Conformational changes in protein loops and helices induced by post-translational phosphorylation. PLoS Comput Biol 2:e32
21. Banavali NK, Roux B (2007) Anatomy of a structural pathway for activation of the catalytic domain of Src kinase Hck. Proteins 67:1096
22. Shah IM, Laaberki MH, Popham DL, Dworkin J (2008) A eukaryotic-like Ser/Thr kinase signals bacteria to exit dormancy in response to peptidoglycan fragments. Cell 135:486
23. Gerhardt P, Marquis RE (1989) Spore thermoresistance mechanisms. In: Smith I, Slepecky RA, Setlow P (eds) Regulation of Prokaryotic Development American Society for Microbiology, Washington, DC, pp 43–63
24. Kazakov S, Bonvouloir E, Gazaryan I (2008) Physicochemical characterization of natural ionic Microreservoirs: *Bacillus subtilis* dormant spores. J Phys Chem B 112:2233
25. Setlow P, Kornberg A (1970) Biochemical studies of bacterial sporulation and germination. XXII. Energy metabolism in early stages of germination of Bacillus megaterium spores. J Biol Chem 245:3637
26. Madec E, Stensballe A, Kjellstrom S, Cladiere L, Obuchowski M, Jensen ON, Seror SJ (2003) Mass spectrometry and site-directed mutagenesis identify several autophosphorylated residues required for the activity of PrkC, a Ser/Thr kinase from *Bacillus subtilis*. J Mol Biol 330:459
27. Johnson LN, Noble ME, Owen DJ (1996) Active and inactive protein kinases: structural basis for regulation. Cell 85:149
28. Wehenkel A, Fernandez P, Bellinzoni M, Catherinot V, Barilone N, Labesse G, Jackson M, Alzari PM (2006) The structure of PknB in complex with mitoxantrone, an ATP-competitive inhibitor, suggests a mode of protein kinase regulation in mycobacteria. FEBS Lett 580:3018
29. Fernandez P, Saint-Joanis B, Barilone N, Jackson M, Gicquel B, Cole ST, Alzari PM (2006) The Ser/Thr protein kinase PknB is essential for sustaining mycobacterial growth. J Bacteriol 188:7778
30. Duran R, Villarino A, Bellinzoni M, Wehenkel A, Fernandez P, Boitel B, Cole ST, Alzari PM, Cervenansky C (2005) Conserved autophosphorylation pattern in activation loops and juxtamembrane regions of Mycobacterium tuberculosis Ser/Thr protein kinases. Biochem Biophys Res Commun 333:858
31. Boitel B, Ortiz-Lombardia M, Duran R, Pompeo F, Cole ST, Cervenansky C, Alzari PM (2003) PknB kinase activity is regulated by phosphorylation in two Thr residues and dephosphorylation by PstP, the cognate phospho-Ser/Thr phosphatase, in Mycobacterium tuberculosis. Mol Microbiol 49:1493
32. Vulpetti A, Bosotti R (2004) Sequence and structural analysis of kinase ATP pocket residues. Farmaco 59:759
33. Pedretti A, Villa L, Vistoli G (2002) VEGA: a versatile program to convert, handle and visualize molecular structure on Windows-based PCs. J Mol Graph Model 21:47
34. Adams JA (2001) Kinetic and catalytic mechanisms of protein kinases. Chem Rev 101:2271
35. Krupa A, Preethi G, Srinivasan N (2004) Structural modes of stabilization of permissive phosphorylation sites in protein kinases: distinct strategies in Ser/Thr and Tyr kinases. J Mol Biol 339:1025
36. Gay LM, Ng HL, Alber T (2006) A conserved dimer and global conformational changes in the structure of apo-PknE Ser/Thr protein kinase from Mycobacterium tuberculosis. J Mol Biol 360:409
37. Nolen B, Taylor S, Ghosh G (2004) Regulation of protein kinases; controlling activity through activation segment conformation. Mol Cell 15:661
38. Shan Y, Seeliger MA, Eastwood MP, Frank F, Xu H, Jensen MO, Dror RO, Kuriyan J, Shaw DE (2009) A conserved protonation-dependent switch controls drug binding in the Abl kinase. Proc Natl Acad Sci USA 106:139
39. Zheng J, Knighton DR, ten Eyck LF, Karlsson R, Xuong N, Taylor SS, Sowadski JM (1993) Crystal structure of the catalytic

subunit of cAMP-dependent protein kinase complexed with MgATP and peptide inhibitor. Biochemistry 32:2154
40. Bossemeyer D, Engh RA, Kinzel V, Ponstingl H, Huber R (1993) Phosphotransferase and substrate binding mechanism of the cAMP-dependent protein kinase catalytic subunit from porcine heart as deduced from the 2.0 A structure of the complex with Mn2 + adenylyl imidodiphosphate and inhibitor peptide PKI(5–24). EMBO J 12:849
41. Noble ME, Endicott JA, Johnson LN (2004) Protein kinase inhibitors: insights into drug design from structure. Science 303:1800
42. Liu Y, Gray NS (2006) Rational design of inhibitors that bind to inactive kinase conformations. Nat Chem Biol 2:358
43. Xu W, Harrison SC, Eck MJ (1997) Three-dimensional structure of the tyrosine kinase c-Src. Nature 385:595
44. Sicheri F, Moarefi I, Kuriyan J (1997) Crystal structure of the Src family tyrosine kinase Hck. Nature 385:602
45. Wood ER, Truesdale AT, McDonald OB, Yuan D, Hassell A, Dickerson SH, Ellis B, Pennisi C, Horne E, Lackey K, Alligood KJ, Rusnak DW, Gilmer TM, Shewchuk L (2004) A unique structure for epidermal growth factor receptor bound to GW572016 (Lapatinib): relationships among protein conformation, inhibitor off-rate, and receptor activity in tumor cells. Cancer Res 64:6652
46. Sheridan RP, Holloway MK, McGaughey G, Mosley RT, Singh SB (2002) A simple method for visualizing the differences between related receptor sites. J Mol Graph Model 21:217
47. Zhou J, Adams JA (1997) Is there a catalytic base in the active site of cAMP-dependent protein kinase? Biochemistry 36:2977
48. Schechter I, Berger A (1967) On the size of the active site in proteases. I. Papain. Biochem Biophys Res Commun 27:157
49. Ortiz-Lombardia M, Pompeo F, Boitel B, Alzari PM (2003) Crystal structure of the catalytic domain of the PknB serine/threonine kinase from Mycobacterium tuberculosis. J Biol Chem 278:13094
50. Madhusudan AkamineP, Xuong NH, Taylor SS (2002) Crystal structure of a transition state mimic of the catalytic subunit of cAMP-dependent protein kinase. Nat Struct Biol 9:273
51. Cox S, Taylor SS (1995) Kinetic analysis of cAMP-dependent protein kinase: mutations at histidine 87 affect peptide binding and pH dependence. Biochemistry 34:16203
52. Cole JL (2007) Activation of PKR: an open and shut case? Trends Biochem Sci 32:57
53. Schwede T, Kopp J, Guex N, Peitsch MC (2003) SWISS-MODEL: an automated protein homology-modeling server. Nucleic Acids Res 31:3381
54. Wang J, Cieplak P, Kollman P (2000) How well does a restrained electrostatic potential (RESP) model perform in calculating conformational energies of organic and biological molecules? J Comput Chem 21:1049
55. Gruszczyński P, Kaźmierkiewicz R, Obuchowski M, Lammek B (2007) Theoretical modeling of PrkCc, serine-threonine protein kinase intracellular domain, complexed with ATP derivatives QSAR. Comb Sci 27:437
56. Case DA, Cheatham TE 3rd, Darden T, Gohlke H, Luo R, Merz KM Jr, Onufriev A, Simmerling C, Wang B, Woods RJ (2005) The Amber biomolecular simulation programs. J Comput Chem 26:1668
57. Homeyer N, Horn AH, Lanig H, Sticht H (2006) AMBER force-field parameters for phosphorylated amino acids in different protonation states: phosphoserine, phosphothreonine, phosphotyrosine, and phosphohistidine. J Mol Model 12:281
58. Narayanan A, Jacobson MP (2009) Computational studies of protein regulation by post-translational phosphorylation. Curr Opin Struct Biol 19:156
59. Sugawara Y, Iwasaki H (1984) Crystal transformation and conformational change of disodium adenosine 5'-triphosphate and the structure of ATP Na2·2H2O. Acta Crystallogr A 40:C68
60. Schaftenaar G, Noordik JH (2000) Molden: a pre- and post-processing program for molecular and electronic structures. J Comput Aided Mol Des 14:123
61. Schmidt M, Baldridge K, Boatz J, Elbert S, Gordon M, Jensen J, Koseki S, Matsunaga N, Nguyen K, Su S, Windus T, Dupuis M, Montgomery J (1993) General atomic and molecular electronic structure system. J Comput Chem 14:1347
62. Bayly CI, Cieplak P, Cornell WD, Kollman PA (1993) A well-behaved electrostatic potential based method using charge restraints for deriving atomic charges: the RESP model. J Phys Chem 97:10269
63. Meagher K, Redman L, Carlson H (2003) Development of polyphosphate parameters for use with the AMBER force field. J Comput Chem 24:1016
64. Morris G, Goodsell D, Halliday R, Huey R, Hart W, Belew R, Olson A (1999) Automated docking using a Lamarckian genetic algorithm and an empirical binding free energy function. J Comput Chem 19:1639
65. Holland J (1992) Adaptation in natural and artificial systems: an introductory analysis with applications to biology, control and artificial intelligence. The MIT Press, Cambridge
66. Sayle RA, Milner-White EJ (1995) RASMOL: biomolecular graphics for all trends. Biochem Sci 20:374
67. Ryckaert J-P, Ciccotti G, Berendsen H (1977) Numerical integration of the cartesian equations of motion of a system with constraints: molecular dynamics of n-alkanes. J Comput Phys 23:327
68. Miyamoto S, Kollman P (1992) SETTLE: an analytical version of the SHAKE and RATTLE algorithm for rigid water models. J Comput Chem 13:952
69. Berendsen HJC, Postma JPM, Vangunsteren WF, Dinola A, Haak JR (1984) Molecular-dynamics with coupling to an external bath. J Chem Phys 81:3684
70. Delano WL (2002) The PyMOL molecular graphics system on World Wide Web http://www.pymol.org